Influence of *In Situ* Compatibilization on *In Situ* Formation of Low-Density Polyethylene/Polyamide 6 Blends by Reactive Extrusion

Hui Fang,[1,2] Guisheng Yang[2,3]

[1]*Department of Materials Science and Engineering, Fujian University of Technology, Fuzhou 350108, People's Republic of China*
[2]*Shanghai Genius Advanced Materials Co., Ltd, Shanghai 201109, People's Republic of China*
[3]*CAS Key Laboratory of Engineering Plastics, Joint Laboratory of Polymer Science and Materials, Institute of Chemistry, Chinese Academy of Sciences, Beijing 100080, People's Republic of China*

Received 2 September 2009; accepted 23 November 2009
DOI 10.1002/app.31843
Published online 4 February 2010 in Wiley InterScience (www.interscience.wiley.com).

ABSTRACT: Low-density polyethylene/polyamide 6 (LDPE/PA6) blends were *in situ* formed by reactive extrusion, in which *in situ* polymerization of ε-caprolactam (CL) and *in situ* copolymerization of maleic anhydride grafted low-density polyethylene (LDPE-MA) and CL took place simultaneously. The latter reaction could be considered as *in situ* compatibilization, and the influence of *in situ* compatibilization on the morphologies, thermal properties, and rheological behaviors of the blends was investigated in this work. Scanning electron microscopy showed that the *in situ* compatibilization could dramatically reduce the dispersed phase sizes and narrow the size distribution. The thermal properties indicated that in differential scanning calorimetry (DSC) cooling scans, fractionated crystallization of the PA6 component was observed in all cases and was promoted with increasing the amount of LDPE-MA. The DSC second heating scans showed the *in situ* compatibilization could stimulate the formation of the less stable γ-crystalline form of PA6 in the blends. Dynamic rheological experiments revealed the *in situ* compatibilization had enhanced the viscosity, storage modulus, and loss modulus of the blend and reduce the corresponding slope values of the storage modulus and loss modulus. © 2010 Wiley Periodicals, Inc. J Appl Polym Sci 116: 3027–3034, 2010

Key words: *in situ* polymerization; *in situ* compatibilization; reactive extrusion; polyamide 6; blend

INTRODUCTION

Compared to the costly synthesis of new homopolymers, blending two or more different polymers is a much more economical approach to obtain new materials. However, the mostly existing polymers used in producing corresponding blends are thermodynamically immiscible, which could lead to high interfacial tension and weak adhesion at the interfaces between the dispersed phases and the matrix. As a result, coarse morphologies and inferior mechanical properties arise. To avoid the aforementioned defects of the blends, compatibilizers seem to be necessary, which could reduce the interfacial tension and help dispersion. Graft copolymer is one of the most popular compatibilizers. Nevertheless, not all graft copolymers could be synthesized by conventional chemical approach for technical and/or economical reasons, and sometimes it is formed during processing, which is called reactive blending, reactive compatibilization, or *in situ* compatibilization.[1]

Blends of polyethylene (PE) and polyamide 6 (PA6) have got particular attention because of the advantages expected from a synergistic match of the low price, good processability, and excellent impact properties of the former resin with the thermal and mechanical properties and oil resistance of the latter.[2–4] At the same time, PE and PA6 exhibit thermodynamically immiscible as well, and then the blends also encounter the above problem. A variety of compatibilizers have been used in PE/PA6 blends for the purpose of achieving a stable system. These copolymers are generally based on premade PE functionalized with maleic anhydride,[5–10] methacrylic acid,[11] acrylic acid,[12] itaconic acid,[13] diethyl succinate,[14] and glycidyl methacrylate,[15] and are typically created by reactive extrusion. Recently, Cartier and Hu[16] reported a novel reactive extrusion process to obtain compatibilized A/B immiscible polymer blends. In their work, a monomer of polymer A was

Correspondence to: G. Yang (ygs@geniuscn.com).
Contract grant sponsor: Shanghai Postdoctoral Sustentation Fund, China; contract grant number: 08R21421500.
Contract grant sponsor: Shanghai Genius Advanced Materials Co., Ltd.

TABLE I
Detailed Compositions and CL Conversion

Sample code	LDPE (g)	LDPE-MA (g)	CL (g)	NaOH (g)	TDI (g)	y^a (%)
B0	1400	0	600	5	4.8	93.5
B5	1300	100	600	6	4.8	92.7
B10	1200	200	600	7	4.8	92.1
B15	1100	300	600	8	4.8	91.4

[a] y is the CL conversion.

incorporated in the presence of polymer B. A fraction of polymer B chains bore some activated groups which could initiate polymer A chain growth. In the process, polymer A and a graft or block copolymer of A and B were formed simultaneously leading to *in situ* polymerization and *in situ* compatibilization of polymer A/B blends.

In this work, LDPE/PA6 blends were prepared by reactive extrusion based on the above approach. Compared with simple blending of LDPE and PA6, the most attractive aspect of this process lay in the following: (1) It requires no consideration about the dispersion of compatibilizers in the matrix, because the compatibilizers are *in situ* formed at the interface of two phases. (2) It allows easier control of the molecular weight of PA6.

In our previous work,[17] the styrene-maleic anhydride (SMA) copolymer had initiated the polymerization of ε-caprolactam (CL) in the blends of SMA-g-PA6/PPO. In this contribution, maleic anhydride grafted low-density polyethylene (LDPE-MA) used as the compatibilizer precursor was adopted in LDPE/PA6 blends by reactive extrusion. The mechanism of the formation of *in situ* compatibilizer, PA6 grafted LDPE (LDPE-g-PA6), was explored. Moreover, the effect of *in situ* compatibilization on the morphologies, thermal properties, and rheological behaviors of the blends was investigated.

EXPERIMENTAL

Materials

LDPE [1C7A, melt flow index = 7.0 g/10 min (190°C, 2.16 kg)] and LDPE-MA [Surbond^{TM} ME21G, melt flow index = 6.0 g/10 min (190°C, 2.16 kg), MA content = 0.8 wt %] used in this study were supplied by SINOPEC Beijing Yanshan Petrochemical Co., Ltd. (P. R. China) and Lianyong plastic technology Ltd. (P. R. China), respectively. The monomer, CL, was purchased from BASF (Germany). Sodium hydroxide (NaOH) and toluene diisocyanate (TDI) were obtained from Shanghai Chemical Reagent Co., Ltd. (Shanghai, P. R. China) (Analysis Grade), and used without further purification. In this work, NaOH was first reacted with CL to obtain sodium ε-caprolactam (sodium-CL) which acted as catalyst, and TDI acted as activator. Other solvents used in this study were all of high purity grade and were used without further purification.

Reactant preparation

The desired amount of CL and NaOH charged into a three-necked flask were first exposed to vacuum at 140°C for 20–25 min to eliminate the water from the absorption and the reaction. When the temperature of the above system declined below 100°C, TDI was added. Meanwhile, the mixture was disturbed for half minute and then pored into a dry box under purging nitrogen gas as soon as possible. Then, the mixture was ground to powder after it cooled down to the room temperature.

Reactive extrusion

Before put into the hopper of the extruder, the aforementioned reactive mixture, LDPE and LDPE-MA were simply premixed, and the detailed compositions were listed in Table I.

The extruder used in this study was an intermeshing co-rotating twin-screw extruder (Nanjing Ruiya Polymer Processing Equipment Co., Ltd., P. R. China) which had 14 barrel sections with electric heaters and water cooling systems. The screw diameter was 35 mm; the distance between two screw axes was 30 mm, and the active barrel length was 2100 mm (L/D = 60). The extruder was operated at 140 to 200°C between the hopper and the second kneading zone and at 240°C for the rest of the screw length and the extrusion die, and at a screw speed of 75 rpm. In addition, the frequency of the feeding motor was set at 3.5 Hz.

Extraction of compatibilizer

To confirm the fact that *in situ* compatibilization took place during reactive extrusion, the compatibilizers were separated from the blends by the following method. First, the blends were extracted with boiling xylene, which was a good solvent for the polyethylene phase, and then the residues were extracted at 50°C with formic acid, which was a good solvent for the polyamide phase. In the case of

the blend B0, where the amount of LDPE-MA is zero, there was no remain after extraction. As for the other three blends, some residues were obtained, which were subjected to be dried in a vacuum oven at 80°C for 24 h.

In addition, to explore the *in situ* compatibilization reaction mechanism, the compatibilizer was obtained by the following solution method as well. First, LDPE-MA was dissolved in boiling xylene until a clear solution was obtained. Subsequently, CL and sodium-CL were added into the solution, and the polymerization of CL was initiated by LDPE-MA under reflux. After about 30 min, some transparent gel can be seen in solution. The obtained gel was filtered, and washed with xylene, formic acid for several times to remove any possible monomer and/or homopolymers. The final product was dried in a vacuum oven at 80°C for 24 h.

Characterization

The IR spectra were recorded by a Fourier transform infrared spectroscopy (FTIR; Nicolet 170SX) onto pressed thin films less than 100 μm in the range 4000–500 cm^{-1} with a resolution of 4 cm^{-1}.

To measure the conversion of CL to PA6, a small amount specimen was first pressed into a thin film about 200 μm. The residual CL was then extracted by Soxhlet extraction for 24 h using ethanol as solvent. Finally the purified film was dried in a vacuum oven at 80°C for 24 h. The nitrogen contents of the films were measured by element analysis (EA; VARIO ELIII). The CL conversion y was calculated by the following equation:

$$y = \frac{N - 0.24\% \times 16.1\%}{30\% \times 12.4\%} \times 100\% \quad (1)$$

with N as the nitrogen content in the polymerized blend after extraction, 0.24% and 30% as the TDI and CL mass content in reactive system respectively, and 16.1% and 12.4% as the nitrogen content in TDI and CL respectively.

To detect whether or not there are small molecules in the polymerized blend after extraction, thermogravimetric analysis (TGA; SDT Q600) was performed on this specimen just mentioned in N_2 atmosphere from 50 to 650°C at heating rate of 10°C/min.

The morphology of the LDPE/PA6 blends was examined by using scanning electron microscopy (SEM; JSM-6360LV) at an acceleration voltage of 10 kV. The cryogenically fractured surfaces were observed after gold sputtering. The SEM photographs were quantitatively analyzed by the counting of the size of the dispersed phase from different fields of the specimen. The number-average diameter (D_n) and volume average diameter (D_v) were calculated from a minimum of 200–300 particles by eqs. (2) and (3), respectively[18,19]:

$$D_n = \frac{\sum_i N_i D_i}{\sum_i N_i} \quad (2)$$

$$D_v = \frac{\sum_i N_i D_i^4}{\sum_i N_i D_i^3} \quad (3)$$

with N_i as the number of particles having diameter D_i. Finally, the size polydispersity d, which is a direct measure of size distribution of the dispersed phase, is calculated as

$$d = D_v/D_n \quad (4)$$

The melting and crystallization behavior of the materials was examined using differential scanning calorimetry (DSC). All the measurements were subjected to the following cycle: the specimens were heated from 50 to 250°C at 20°C/min, held at 250°C for 5 min to erase any previous thermal history, then cooled down to 50°C at 10°C/min (crystallization) and heated again to 250°C at 10°C/min (melting).

Rheological measurements were made in dynamic mode on a rotational rheometer (ARES rheometer; Rheometric Scientific) equipped with parallel plate geometry (plate diameter 25 mm). Sheets were compression molded to about 1 mm thickness and punched into disks of 25 mm diameter. Dynamic frequency scan tests were conducted for all samples at a strain sweep of 5% at 230°C.

RESULTS AND DISCUSSION

In situ polymerization and *in situ* compatibilization reaction schemes

During the reactive extrusion in this study *in situ* polymerization and *in situ* compatibilization take place simultaneously, so the reaction scheme is concerned with the formation of PA6 homopolymer and LDPE-g-PA6 copolymer.

Figure 1 shows schematically the reactions of *in situ* polymerization and *in situ* compatibilization. On the one hand, the CL is polymerized into PA6 via anionic ring-opening polymerization of CL in the presence of a catalyst (sodium-CL) and an activator bearing isocyanate group (TDI). On the other hand, the MA grafted on LDPE reacts firstly with sodium-CL to form acyl caprolactam, and then LDPE bearing acyl caprolactam acts as a macro-activator initiating the polymerization of CL, which results in the formation of LDPE-g-PA6 copolymer.

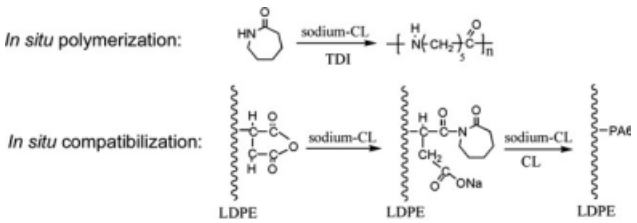

Figure 1 Reaction schemes of *in situ* polymerization and *in situ* compatibilization.

To confirm the *in situ* compatibilization reaction mechanism, the compatibilizer obtained by solution method is subjected to the FTIR measure. For comparison, the spectra of the LDPE-MA and compatibilizer extracted from the blend B15 are exhibited as well. As can be detected in Figure 2, the peak at 1784 cm^{-1} characteristic absorption stretching vibration of the carbonyl group in maleic anhydride disappears and two new peaks appear in the compatibilizer obtained by solution method. The peaks at 1633 and 1540 cm^{-1} are corresponding to the C=O stretching vibration and the N—H bending vibration of the amide[20] in PA6, respectively. It is suggested that the compatibilizer obtained by solution method is LDPE-g-PA6 copolymer. On the other hand, the compatibilizer extracted from the blend B15 exhibits similar IR spectra with that obtained by solution method, which means that the former was LDPE-g-PA6 compatibilizer as well, and the *in situ* compatibilization had taken place during reactive extrusion.

CL conversion

In the work of Zhang et al.,[21] four methods of measuring the conversion of CL to PA6 were introduced. AS some CL monomers could be exhausted from the

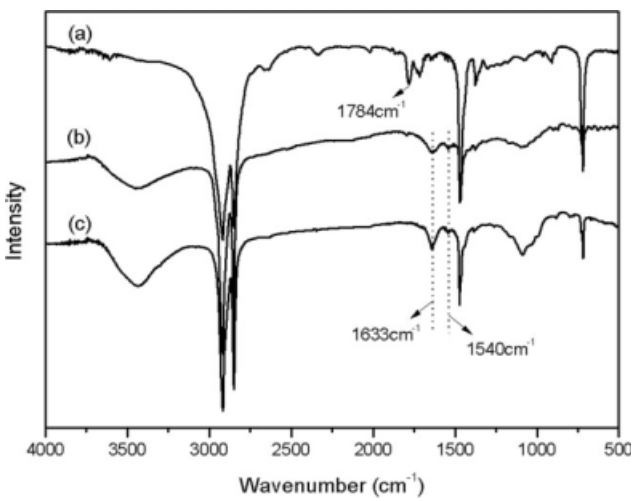

Figure 2 FTIR spectra: (a) LDPE-MA, (b) LDPE-g-PA6 obtained by solution method, and (c) LDPE-g-PA6 extracted from the blend B15.

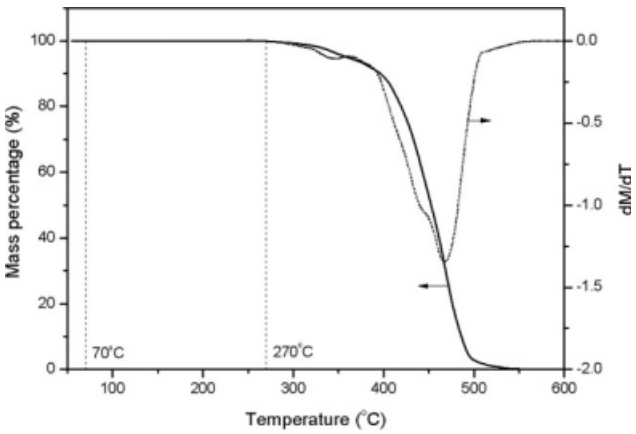

Figure 3 TGA diagram of the blend B5 extracted in ethanol.

venting port and the die during reactive extrusion, the method of EA for the nitrogen contents was adopted in this work. To estimate whether or not there are small molecules the polymerized blend after extraction in ethanol, TGA was performed. Figure 3 shows the TGA trace of the blend B5 which had been subjected to ethanol extraction and then vacuum drying at 80°C for 24 h. It is seen that there is no mass lost in the temperature range between 70 and 270°C, which indicates that CL residue and ethanol have been completely removed. Therefore, the actual CL conversion can be defined by EA and the results are listed in Table I. In all cases, there is little difference among the CL conversions of the blends, and the values are greater than 90%, which suggests that the *in situ* formation of LDPE/PA6 blends by reactive extrusion is feasible.

Morphology of the polymerized blends

Figure 4 shows the SEM photographs of the polymerized blends and Table II shows the particle (PA6 phase) size and size polydispersity obtained from these photographs. In all blends, the dispersive phase (PA6) as spherical particles immersed in the continuous matrix (LDPE). With increasing the amount of LDPE-MA, the particle size for the corresponding blend declines and the particle size distribution becomes narrow. Additionally, in all cases, there exist small spheres with the diameter about 400 nm or more less.

The above observation suggests that LDPE and PA6 exhibit thermodynamically immiscible. As for the small spheres in all blends, it is contributed to the morphological evolvement in the reactive extrusion, which is different from that in the classical processing for a direct mixture of two polymers. During the reactive extrusion, the CL monomers were initially dispersed into small droplets and subsequently polymerized to PA6 particles, and then

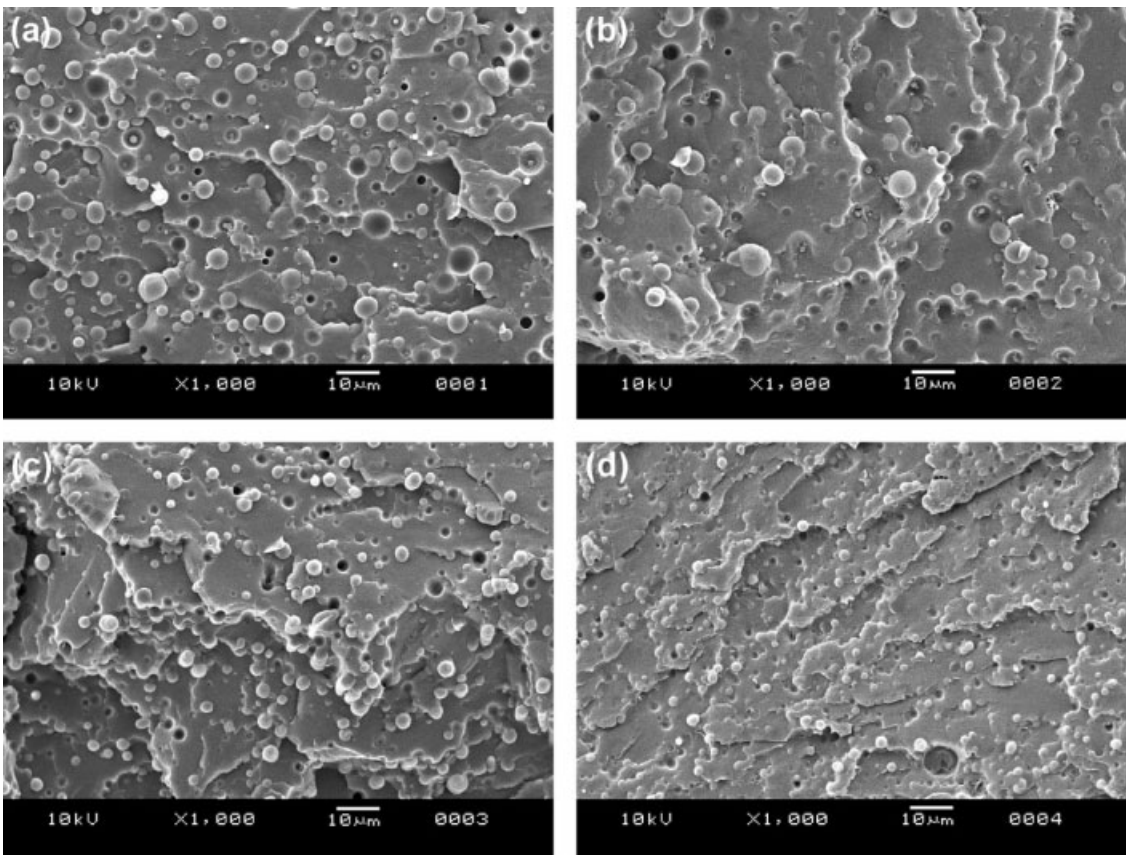

Figure 4 SEM photographs of the LDPE/PA6 blends: (a) B0, (b) B5, (c) B10, and (d) B15.

with the blending, some of the spheres might keep the small sizes but the others might become larger due to coalescence. However, as LDPE-MA was introduced, to some extent, the LDPE-g-PA6 *in situ* formed could stabilize the initial sphere size and cause a reduction in the probability of coalescence, and consequently smaller dispersed phase sizes and narrower size distribution.

Analysis of thermal properties

Figures 5 and 6 show DSC cooling and second heating scans for LDPE/PA6 blends and Table III summarizes the calorimetric data measured from these figures. The crystallization temperature (T_c) and melting temperature (T_m) values for LDPE and LDPE-MA are reported as well.

TABLE II
Particle Size and Size Polydispersity Calculated from SEM Photographs

Sample code	D_v (μm)	D_n (μm)	d
B0	3.89	2.50	1.56
B5	3.48	2.41	1.44
B10	2.53	2.07	1.22
B15	1.71	1.48	1.16

The cooling scans shown in Figure 5 exhibit several exotherms for all of the blends during cooling runs, which indicates that LDPE-MA introduced could affect the cooling behaviors of the blends. As can be seen in Table III, compared with the pure LDPE and LDPE-MA, the T_c of the LDPE component in the reactive blends shifted in all cases, to higher values, and it is suggested that the LDPE component

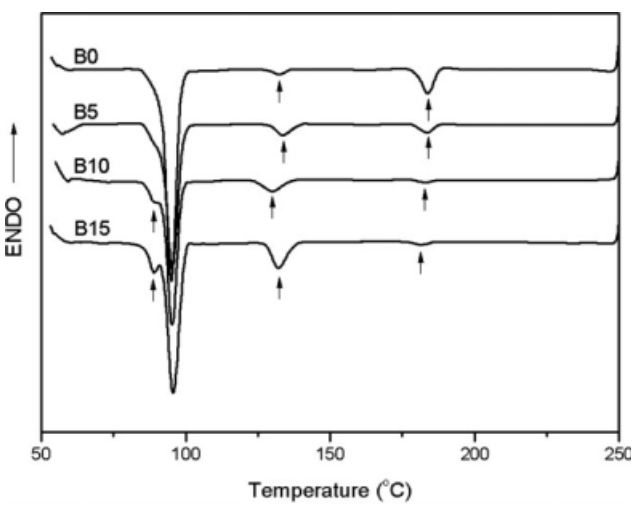

Figure 5 DSC cooling scans at 10°C/min for the LDPE/PA6 blends.

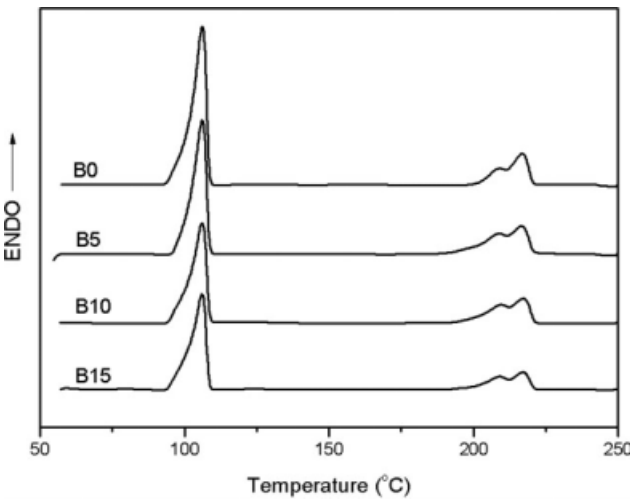

Figure 6 DSC second heating scans at 10°C/min for the LDPE/PA6 blends.

could be nucleated by the PA6 component. Additionally, the fractionated crystallization of PA6 component in all blends is observed, which is indicated in Figure 5 with arrows that signaled the two or three crystallization exotherms. Table III lists all the crystallization temperatures. As the literatures reported,[22–25] fractionated crystallization occurs when the number of heterogeneous nuclei of the bulk crystallizable polymer, which usually active at low undercoolings, is lower than the number of dispersed droplets of this polymer in the blend. Those particles without the nuclei could crystallize followed homogeneous nucleation mechanism at higher undercoolings. This means that fractionated crystallization proceeds stepwise at increasing undercoolings, depending on the level of dispersion. In addition, it should be mentioned that fractionated crystallization process in the blends seems not to be due to *in situ* compatibilization, but a consequence of the dispersion level of the minor phase. This was ascertained because the same effect was observed in the blend B0 without LDPE-MA. However, the more LDPE-MA is introduced, the sharper the fractionated crystallization peaks at the low temperatures (about 88 and 132°C) are. This is reasonable because a finer and more homogeneously dispersed morphology of PA6 phase is obtained with increasing the amount of LDPE-MA, which leads to the crystallization of the PA6 component shifting to the lower temperature.

On the other hand, as shown in Figure 6, in all blends, double melting peaks (about 209 and 217°C) appear in the PA6 component, which may be ascribed to the melting peaks of the γ-crystalline form and α-crystalline form of PA6, respectively. The α-crystalline form posses a better stability, while the γ-crystalline form is less stable.[26,27] Furthermore, it seems that there is more γ-crystalline form as the amount of LDPE-MA increased. It can be explained that the fractionated crystallization of the PA6 component in the blends promotes a higher amount of the less stable γ-crystalline form under the confining conditions at which they are formed.

Analysis of rheological properties

Generally, the rheological behavior of polymer blends is influenced by several factors such as the miscibility of the system, the morphology, the interfacial adhesion, and the interfacial thickness.[28] In immiscible systems having separated phases, as shown in our case by the morphological observations and thermal properties, it is important to consider the influence of the morphology on the rheological properties of the systems, moreover, in a compatibilized system that could have a third phase with its own rheological characteristics.

Figure 7 shows double logarithmic plots of complex viscosity (η*), storage modulus (G'), and loss modulus (G'') as functions of frequency (ω) for the blends. It is apparent that the *in situ* compatibilization has dramatic effects on the rheological behavior of the blends.

As shown in Figure 7(a), each blend exhibits a thixotropic behavior (shear thinning), and with increasing the amount of LDPE-MA, the η* increases over the entire frequency range. This contributes to

TABLE III
Thermal Characterization of the LDPE/PA6 Blends

	LDPE		PA6		LDPE	PA6[a]	
Sample code	T_c (°C)		T_c (°C)		T_m (°C)	T_{m1} (°C)	T_{m2} (°C)
LDPE	91.4	–	–	–	106.0	–	–
LDPE-MA	89.0	–	–	–	104.0	–	–
B0	95.0	–	132.5	183.9	106.1	209.0	216.8
B5	95.2	–	133.6	183.7	106.0	209.0	217.4
B10	95.3	88.8	130.0	182.9	105.9	209.6	217.3
B15	95.7	88.8	132.1	182.3	105.9	209.1	218.0

[a] T_{m1} and T_{m2} are attributed to the two melting peaks of the PA6.

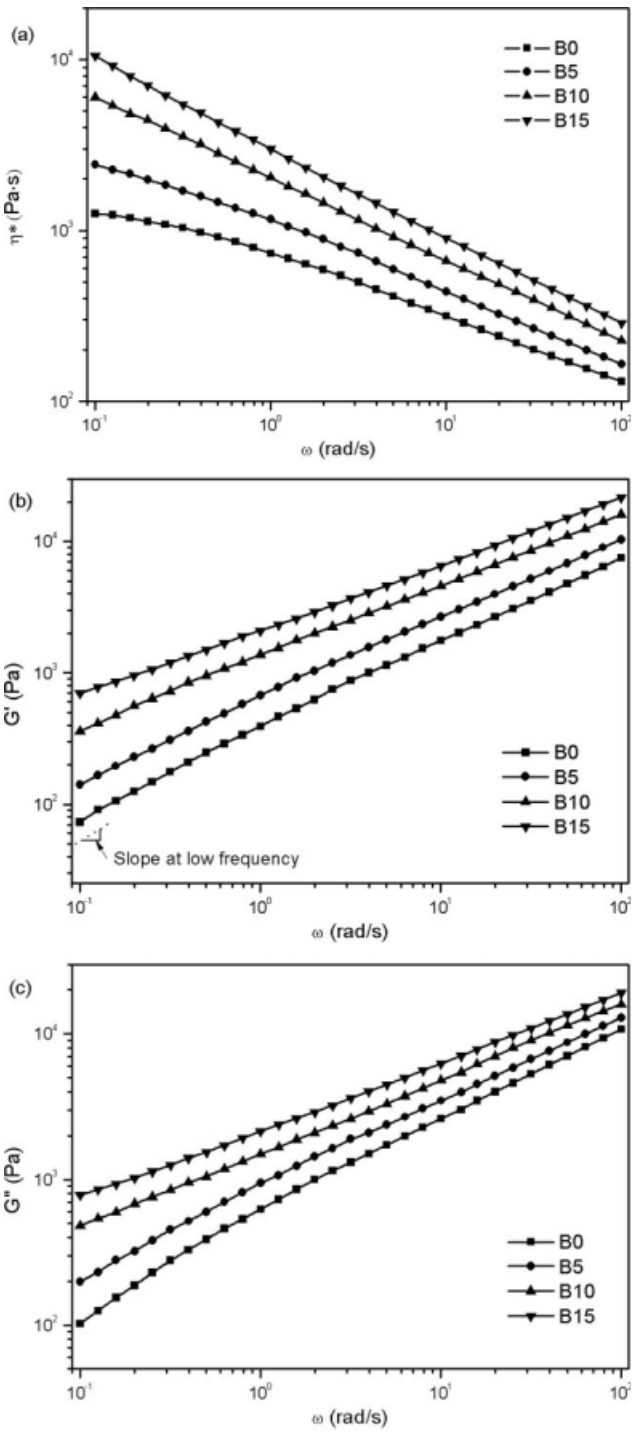

Figure 7 Rheological properties of the blends: (a) η*, (b) G', and (c) G'' vs ω. Note: this figure also indicates how the slope at low frequency is determined.

the *in situ* formed LDPE-g-PA6 compatibilizers, which were located at the interface between the two phases, leading to an enhancement in the interfacial adhesion and therefore to an increase in the viscosity.[28]

The increase in the viscosity is caused by a similar increase in G' and G''. As can be seen in Figure 7(b,c), with increasing the amount of LDPE-MA, the corresponding blend shows higher G' and G'' values. In addition, Table IV lists the slope values of both G' and G'' at low frequency (at 0.1 rad/s). Alterations in the slope values of G' and G'' at terminal zone (low frequencies) are likely to reflect the blend compatibility. In general, a lower slope value at low frequency suggests that there is a shorter relaxation process caused by a stronger blend interphase, which means improved compatibility. Consequently, the LDPE-MA introduced in the system can lead to *in situ* formation of LDPE-g-PA6 which promotes the compatibility of the blend, resulting from the decline in the slope values with increasing the amount of LDPE-MA.

CONCLUSIONS

In this work, LDPE/PA6 blends were prepared by reactive extrusion, where *in situ* polymerization and *in situ* compatibilization took place simultaneously resulting in the formation of PA6 homopolymer and LDPE-g-PA6 copolymer. By means of the characterization of the LDPE-g-PA6 copolymers obtained by solution method and extraction from the blend, the *in situ* compatibilization reaction mechanism induced by LDPE-MA was confirmed.

As shown in the SEM photographs, there were some tiny dispersed particles in the blends, even in the case of the blend B0. It was contributed to the morphological evolvement in the reactive extrusion, where the CL monomers were initially dispersed into small droplets and subsequently polymerized to small-sized PA6 particles. As LDPE-MA was introduced, the LDPE-g-PA6 *in situ* formed was helpful to stabilize the initial sphere size and cause a reduction in the probability of coalescence, and consequently smaller dispersed phase sizes and narrower size distribution.

The thermal properties showed some changes due to *in situ* compatibilization. In DSC cooling scans, fractionated crystallization of the PA6 component was observed in all cases and was promoted with increasing the amount of LDPE-MA. Additionally, nucleation of the LDPE component by the PA6 component was observed for all of the blends. The DSC

TABLE IV
The Slope Values of G' and G'' at Low Frequency (0.1 rad/s)

Sample code	Slope of G'	Slope of G''
B0	0.93	0.90
B5	0.74	0.68
B10	0.59	0.50
B15	0.46	0.38

Note: The determination of the slope is indicated in Figure 7.

second heating scans showed the presence of two crystalline forms of PA6 in the blends, and the *in situ* compatibilization could stimulate the formation of the less stable γ-crystalline form.

Dynamic rheological experiments revealed a noticeable shifting of the viscosity of the blends to higher values with adding more LDPE-MA, which indicates the *in situ* formed LDPE-g-PA6 compatibilizers located at the interface between the two phases, leading to an enhancement in the interfacial adhesion. The storage modulus and loss modulus exhibited the similar change with the viscosity, and moreover, their slope values at low frequency declined as the amount of LDPE-MA increased, which is due to the improvement of the compatibility of the two phases.

References

1. Baker, W.; Scott, C.; Hu, G. H. Reactive Polymer Blending; Hanser: Munich, 2001.
2. Chen, C. C.; Fontan, E.; Min, K.; White, J. L. Polym Eng Sci 1988, 28, 69.
3. Willis, J. M.; Favis, B. D. Polym Eng Sci 1988, 28, 1416.
4. Koulouri, E. G.; Georgaki, A. X.; Kallitsis, J. K. Polymer 1997, 38, 4185.
5. Gadekar, R.; Kulkarni, A.; Jog, J. P. J Appl Polym Sci 1998, 69, 161.
6. Jurkowski, B.; Kelar, K.; Ciesielska, D. J Appl Polym Sci 1998, 69, 719.
7. Kelar, K.; Jurkowski, B. Polymer 2000, 41, 1055.
8. Jurkowski, B.; Olkhov, Y. A.; Kelar, K.; Olkhova, O. M. Eur Polym J 2002, 38, 1229.
9. Li, J.; Liang, M.; Guo, S. Y.; Kuthanová, V.; Hausnerová, B. J Polym Sci Part B: Polym Phys 2005, 43, 1260.
10. Chatreenuwat, B.; Nithitanakul, M.; Grady, B. P. J Appl Polym Sci 2007, 103, 3871.
11. Valenza, A.; Geuskens, G.; Spadaro, G. Eur Polym J 1997, 33, 957.
12. Fang, Z.; Xu, Y.; Tong, L. Polym Eng Sci 2007, 47, 551.
13. Pesetskii, S. S.; Krivoguz, Y. M.; Jurkowski, B. J Appl Polym Sci 2004, 92, 1702.
14. Geppi, M.; Forte, C.; Passaglia, E.; Mendez, B. Macromol Chem Phys 1998, 199, 1957.
15. Wei, Q.; Chionna, D.; Pracella, M. Macromol Chem Phys 2005, 206, 777.
16. Cartier, H.; Hu, G. H. Polymer 2001, 42, 8807.
17. Du, L. B.; Yang, G. S. J Appl Polym Sci 2008, 108, 3419.
18. Abacha, N.; Fellahi, S. Macromol Symp 2002, 178, 131.
19. Lomellini, P.; Matas, M.; Favis, B. D. Polymer 1996, 37, 5689.
20. Li, L. J.; Yang, G. S. Polym Int 2008, 57, 1226.
21. Zhang, C. L.; Feng, L. F.; Hu, G. H. J Appl Polym Sci 2006, 101, 1972.
22. Santana, O. O.; Müller, A. J. Polym Bull 1994, 32, 471.
23. Morales, R. A.; Arnal, M. L.; Müller, A. J. Polym Bull 1995, 35, 379.
24. Arnal, M. L.; Matos, M. E.; Morales, R. A.; Santana, O. O.; Müller, A. J. Macormol Chem Phys 1998, 199, 2275.
25. Frensch, H.; Jungnickel, B. J. Colloid Polym Sci 1989, 264, 16.
26. Khanna, Y. P. Macromolecules 1992, 25, 3298.
27. Murthy, N. S.; Aharoni, S.; Szollosi, A. J Polym Sci Part B: Polym Phys 1985, 23, 2549.
28. George, S.; Ramamurthy, K.; Anand, J. S.; Groeninckx, G.; Varughese, K. T.; Thomas, S. Polymer 1999, 40, 4325.